Iranian Journal of Oil & Gas Science and Technology, Vol. 4 (2015), No. 3, pp. 37-50
http://ijogst.put.ac.ir

Determination of Pore Pressure from Sonic Log: a Case Study on One of Iran Carbonate Reservoir Rocks

Morteza Azadpour and Navid Shad Manaman*

Department of Petroleum Exploration Engineering, Faculty of Mining Engineering, Sahand University of Technology, Tabriz, Iran

Received: March 06, 2015*; revised:* June 13, 2015*; accepted:* June 20, 2015

Abstract

Pore pressure is defined as the pressure of the fluid inside the pore space of the formation, which is also known as the formation pressure. When the pore pressure is higher than hydrostatic pressure, it is referred to as overpressure. Knowledge of this pressure is essential for cost-effective drilling, safe well planning, and efficient reservoir modeling. The main objective of this study is to estimate the formation pore pressure as a reliable mud weight pressure using well log data at one of oil fields in the south of Iran. To obtain this goal, the formation pore pressure is estimated from well logging data by applying Eaton's prediction method with some modifications. In this way, sonic transient time trend line is separated by lithology changes and recalibrated by Weakley's approach. The created sonic transient time is used to create an overlay pore pressure based on Eaton's method and is led to pore pressure determination. The results are compared with the pore pressure estimated from commonly used methods such as Eaton's and Bowers's methods. The determined pore pressure from Weakley's approach shows some improvements in comparison with Eaton's method. However, the results of Bowers's method, in comparison with the other two methods, show relatively better agreement with the mud weight pressure values.

Keywords: Pore Pressure, Well-logging, Weakley's Approach, Eaton's Method, Carbonate Reservoirs

1. Introduction

Pore pressure is commonly estimated based on well log analysis in combination with Terzaghi's relationship. Based on this relation, the overburden load is dependent on pore pressure and vertical effective stress. This relationship is proposed by Terzaghi (1943) as follows:

$$S = P + \sigma \tag{1}$$

where, S is the overburden pressure (the combine weights of formation solid and fluid); σ is the vertical effective stress (the grain-to-grain contact stress) and P represents the pore pressure.

Pore pressure is defined as the pressure of the fluid inside the pore space of the formation, which is also known as the formation pressure. Based on the magnitude of pore pressure, it can be described as being either normal or abnormal. When the pore pressure is equal to hydrostatic pressure, it is referred

* Corresponding Author:
Email: shmanaman@ut.ac.ir

to as normal pore pressure. Formations with normal pressure are connected to a free surface through the permeable sediments. Abnormal pore pressure addresses the pore pressure which is higher (overpressure) or lower (under pressure) than hydrostatic pressure (Swarbrick et al., 1998). Overpressure can make many problems such as wellbore instability, mud loss, kicks, and blowouts. Overpressure is generated due to different mechanisms such as compaction disequilibrium, unloading due to fluid expansion, chemical digenesis, buoyancy effect, and lateral transfer. Each mechanism affects increasing pressure in a significant way. Therefore, accurate pore pressure determination is necessary for a safe and economic drilling.

2. Pore pressure prediction methods

So far, different methods have been proposed on pore pressure prediction. Hottman and Johnson (1965) conducted the first study on the pore pressure prediction using shale properties derived from well log data. In this way, any deviation in the measured properties from the normal trend line was used as a sign of abnormal pore pressure. Afterwards, other researchers have successfully used resistivity, sonic transit time, porosity, and other well log data for pore pressure prediction. Most of these studies are based on this assumption that any changes in an area with normal pore pressure lead to a change in some petrophysical properties such as compaction, porosity, and fluid motion. Therefore, any measurable parameters, which can somehow show these changes, can be used in the interpretation and quantitative evaluation of pore pressure (Azadpour et al., 2015). Eaton's, Bowers's, and Holbrook's methods have commonly been used in the oil industry for pore pressure prediction.

Eaton's method is one of the conventional methods of the pore pressure prediction, which considers compaction disequilibrium as the main mechanism of overpressure generations. Eaton (1975) proposed an empirical equation to quantify the pore pressure using well log data. This method assumes that overburden pressure is supported by pore pressure and vertical effective stress, as shown in Terzaghi's equation. According to Equation 1, Eaton presented the following empirical equation for pore pressure prediction from sonic transit time:

$$G_p = G_o - (G_o - G_n)\left(\frac{\Delta t_n}{\Delta t_o}\right)^x \tag{2}$$

where, G_p, G_o, and G_n are the pore pressure gradient, the overburden pressure gradient, and the hydrostatic pressure gradient respectively; Δt_o stands for the measured sonic transit time by well logging and Δt_n is the normal sonic transit time in shale obtained from normal trend line; x represents the exponent constant.

Bowers's method is based on the effective stress, which used Terzaghi's equation in pore pressure prediction. The main step in this method is to calculate the effective stress from velocity and then use the Terzaghi's equation in pore pressure calculation. This method considers compaction disequilibrium and unloading due to fluid expansion as the main mechanisms of overpressure generations. In compaction disequilibrium conditions, Bowers (1995) proposed an empirically determined method to calculate the effective stress as follows:

$$V = V_0 + A\sigma^B \tag{3}$$

where, V is the velocity at a given depth and V_0 stands for the surface velocity (normally 1500 m/sec); σ represents the vertical effective stress; A and B are the parameters obtained from calibrating regional

offset velocity versus effective stress data. In unloading conditions, Bowers (1995) proposed the following empirical relation:

$$V = V_0 + A\left[\sigma_{max}\left(\frac{\sigma}{\sigma_{max}}\right)^{\left(\frac{1}{U}\right)}\right]^B \tag{4}$$

$$\sigma_{max} = \left(\frac{v_{max} - 1500}{A}\right)^{\frac{1}{B}} \tag{5}$$

Where, U is the unloading parameter, which is a measure of how plastic the sediment is. U = 1 implies no permanent deformation and U=∞ corresponds to a completely irreversible deformation. σ_{max} and V_{max} represent the values of effective stress and velocity at the onset of unloading, which are maximum, respectively (Bowers, 1995).

Holbrook (1995) also proposed a pore pressure estimation method for naturally fractured reservoirs. There is no need to set any trend lines in Holbrook's method, because this method is based on the relationship between the porosity, mineralogy, and effective stress in granular sedimentary rocks. Holbrook successfully used this effective stress-law in the North Sea to predict pore pressure in limestone, shaly limestone, and sandstone intervals (Holbrook, 1999). Holbrook's method uses the following equation to calculate the effective stress of the rock:

$$\sigma = \sigma_{max} \times (1 - \emptyset)^{\beta} \tag{6}$$

where, σ_{max} is the maximum effective stress required to reduce the mineral porosity to zero and $\emptyset$ is porosity from well logs; β stands for the compaction strain-hardening coefficient for the type of minerals.

Compressibility method, as a new method of pore pressure prediction, was first proposed by Atashbari (2012). He used rock porosity and compressibility to calculate the pore pressure. Any change in pore spaces due to abnormal pressure is a function of bulk and pore volume compressibility. Hence Atashbari (2012) used bulk and pore volume compressibility as parameters to calculate the pore pressure as given below:

$$P = \left(\frac{(1 - \emptyset)C_b\ \sigma_{eff}}{(1 - \emptyset)C_b - \emptyset\ C_p}\right)^{\gamma} \tag{7}$$

where, P_p, fractional ø, C_b (psi^{-1}), and C_p (psi^{-1}) are the pore pressure, porosity, bulk compressibility, and pore compressibility respectively. σ_{eff} (psi) is the effective overburden pressure (overburden pressure-hydrostatic pressure) and χ is an empirical constant ranging from 0.9 to 1.0.

Afterward, Azadpour (2015) proposed a modified form of the above equation based on pore volume compressibility as follows:

$$P = \left(\frac{(1 - \emptyset)C_p\sigma_{eff}}{(1 - \emptyset)C_p - \emptyset\ C_p}\right)^{\gamma} \tag{8}$$

3. Weakley's approach

Pore pressure determinations from log properties in carbonate environments have always faced problems due to the geological complexity in carbonate environments. They do not compact uniformly with depth as do shales. Indeed, the application of common pore pressure prediction

methods to carbonate rocks cannot always yield a right prediction. Weakley (1990) has developed an approach toward determining the formation pore pressures in carbonate environments utilizing sonic velocity trends. He used Eaton's concept, but employed the sonic wave velocity trends for each formation section. These formation sections were detected from well log responses as the lithology changing index. Joining the last value of interval velocity trend from the last lithology section with the first value in the next made a smooth continuous sonic velocity log, which was used in the estimation of pore pressure by applying Eaton's method. The most effective parameters in Eaton's method are the detection of normal compaction trend line, normal compaction trend (NCT), and appropriate exponent constant *x*, which is originally 3 in Eaton's study and requires modification to be implemented in tight unconventional reservoirs (Contreras et al., 2011). Below, some examples of Eaton's exponent less than 3 show this modification in different reservoir formations:

1- x = 0.5 (Azadpour et al., 2015); pore pressure prediction and modeling using well-log data in one of the gas fields in the south of Iran;
2- x = 1 (Contreras et al., 2011); a case study for pore pressure prediction in an abnormally sub-pressured western Canada sedimentary basin;
3- x = 1-1.5 (Yully P. Solano et al., 2007); a modified approach toward predicting pore pressure using the *d*-exponent method;
4- x = 2.6 (Jeff C. Kao et al., 2010); estimating pore pressure using compressional and shear wave data from multicomponent seismic nodes in Atlantis field, the deep-water gulf of Mexico;
5- x = 0.1-0.3 (T. Kadyrov et al., 2012); sonic log-derived pore pressure prediction in a west Kazakhstan dolomite field.

Normal compaction trend line needs to be determined through the normally pressured and normally compacted section of the well log data. Any deviation from the normal trend line indicates the abnormal pressure. To determine the exponent constant, *x*, Eaton's equation is written in terms of *x* as given by:

$$x = \frac{log\left(\frac{G_o - G_p}{G_o - G_n}\right)}{log\left(\frac{\Delta t_n}{\Delta t_o}\right)} \tag{9}$$

Using a known abnormal pore pressure data, the exponent constant *x* is determinable.

4. Case study

The studied oil field is located in the south of Iran. The reservoir formations are composed of shale, marl, anhydrite, dolomite, and limestone. The studied formation sequence includes Asmari, Pabdeh, Gurpi, Ilam, and Sarvak formations. Asmari is a hard limestone formation of Oligocene-Early Miocene, which contains gray and red marl layers with some thin layers of anhydrite in the upper part. Pabdeh formation, of Late Paleocene-Early Oligocene age, contains gray shales, clay limestone, and gray marl and contains pelagic facies. Gurpi is a formation in Late Cretaceous, which consists of more shale, marl limestone, and gray marl. Ilam and Sarvak formations in the studied field are mainly composed of clay limestone, including mudstone, wackstone, and packstone. The porosity is relatively weaker than Asmari formation.

Data from 2 wells, including different petrophysical logs such as sonic transient time, gamma-ray, and density logs (Figure 1) along with mud weight pressure data are used in this study to determine the

pore pressure. Bad data in cases of obvious noise such as cycle skips on the sonic log or hole washouts are corrected. Also, the environmental effects such as wellbore caving, mud salinity, mud pressure, and mud cake are corrected by software. The aim of this study is to evaluate pore pressure within carbonate reservoirs by applying Weakley's approach and comparing the results with pore pressure prediction from usual Eaton's method.

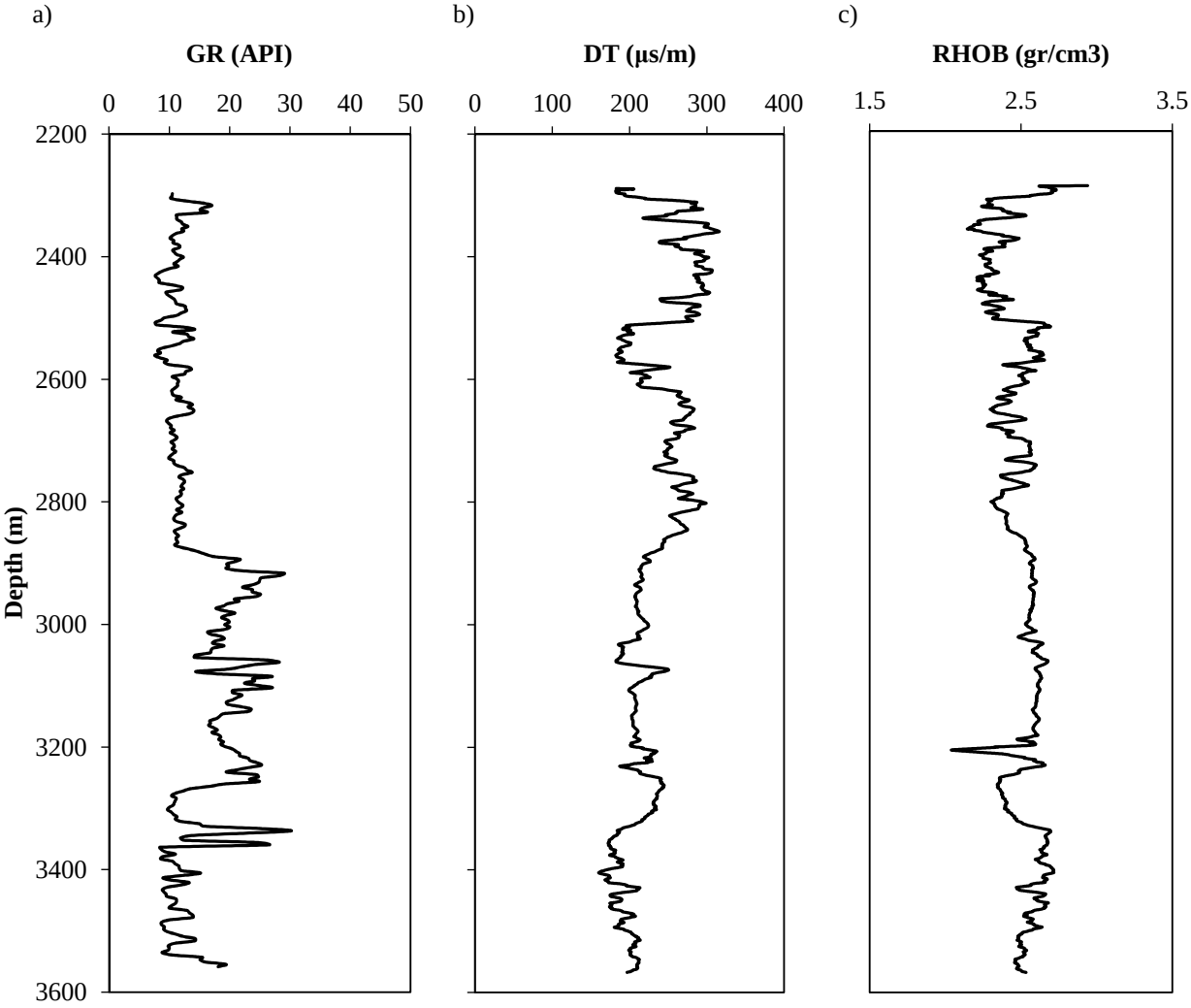

Figure 1
Petrophysical well-log data in the studied well; a) gamma ray log, b) sonic transient time log, and c) density log.

The first step in Weakley's approach is determining lithology tops. This is done by separating different lithologies using gamma ray, density, and sonic logs. Lithology tops are determined by picking the points where the gamma ray, density, or sonic logs shows a change in the general trend. Within lithological sections, the gamma ray peaks were analyzed and showed a trend to the right in the shale direction. The sonic velocities, which correspond to the gamma ray peaks, are detected. Trend lines have been drawn with respect to these sonic velocities peaks as shown in Figure 2. Based on Weakley's approach, sonic trend lines are recalibrated by shifting them at the lithology changes by joining the last value of interval velocity in the last lithological section with the first value in the next. This recalibrates the results in a continuous relative interval sonic transient time (DT) as depicted in Figure 3.

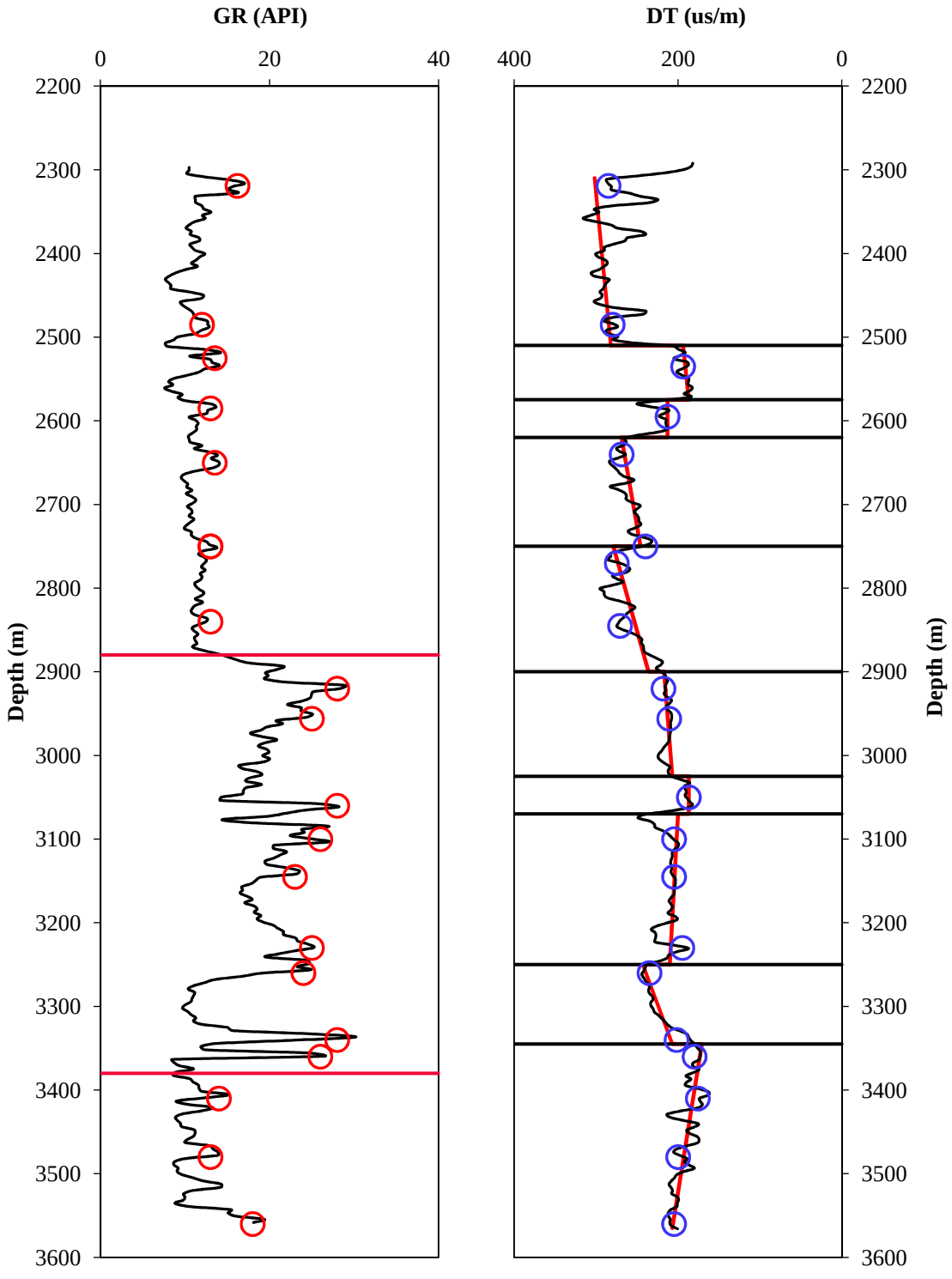

Figure 2
Lithology separations based on changes in petrophysical properties (GR, DT, and RHOB); trend lines are detected based on gamma ray peaks trend to the right for each lithology section.

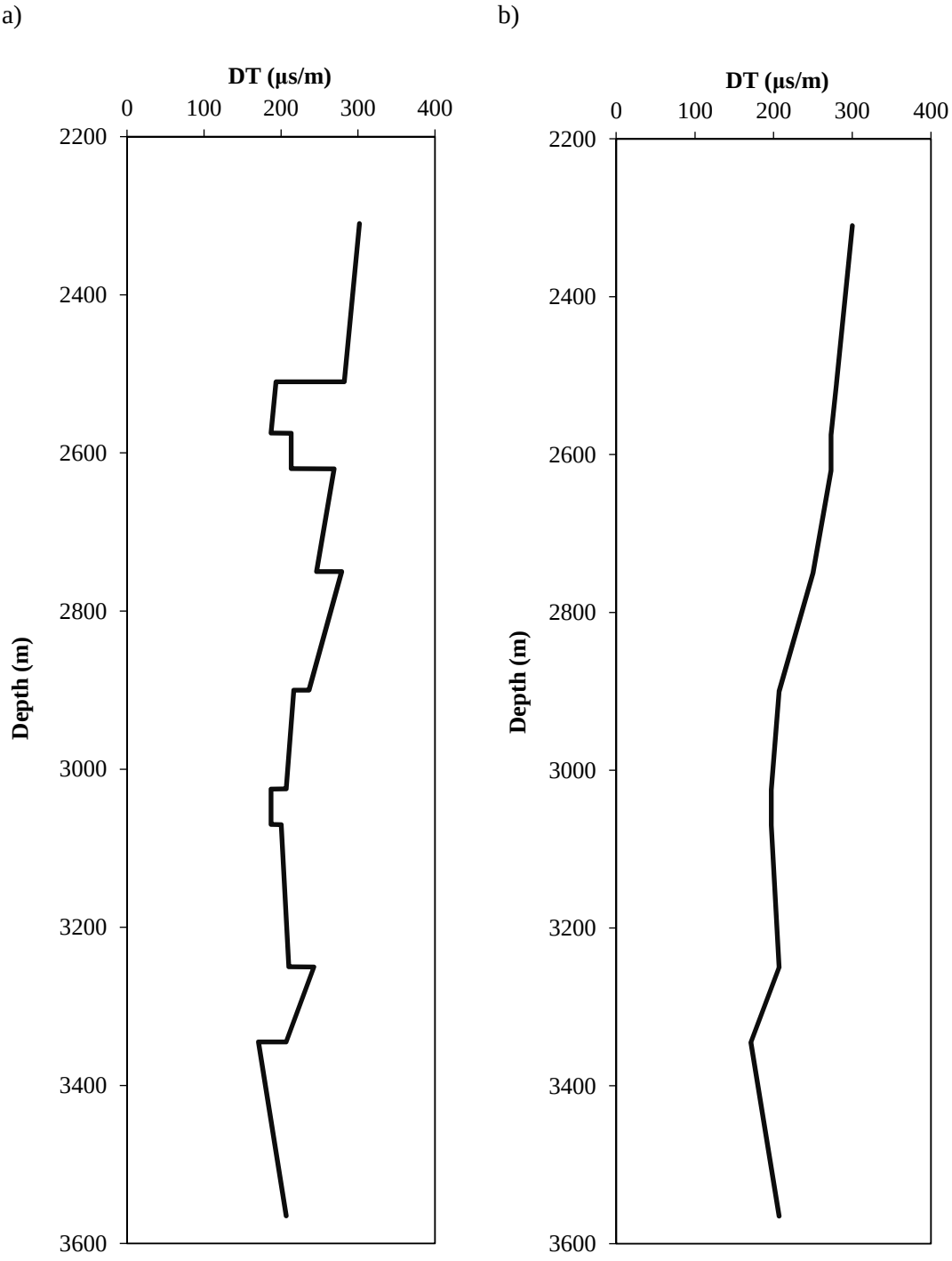

Figure 3
Sonic transient time calibration with Weakley's approach; a) DT log and trend lines within lithologies and b) recalibrated DT trend lines.

The normal DT compaction trend line is detected based on the DT value at the surfaces (660 µs/m) and at the normal pressure depths (2900-3050 m) as shown in Figure 4 with a longer line. Using the bulk density log and average density of 231 gr/cm^3, the average of overburden pressure gradient is determined to be 2233 kPa/m.

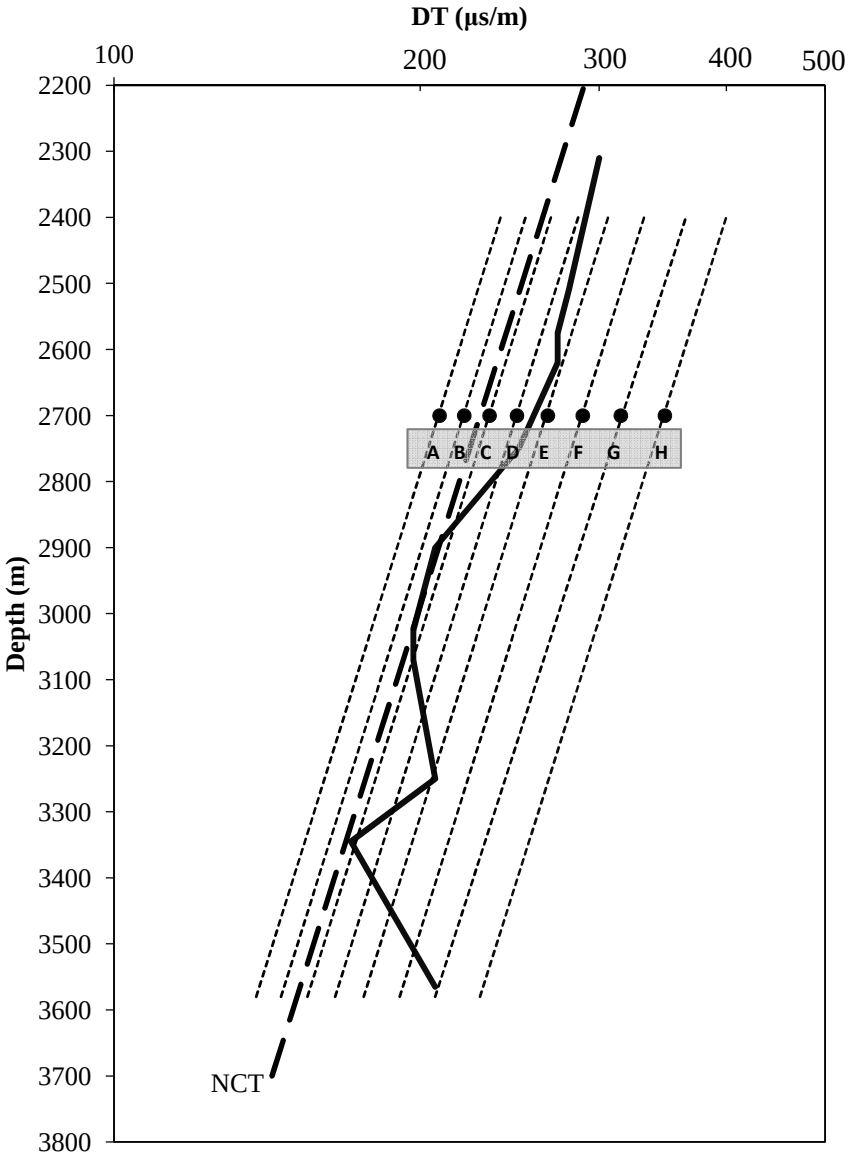

Figure 4
Creating pore pressure over layer in a semi-log plot sheet.

According to the overall studies in the Middle East, especially in Iran, the gradient of normal hydrostatic pressure (G_n) is 10.5 kPa/m (Atashbari et al., 2015). Substituting the determined hydrostatic and overburden pressure gradient in Equation 2, Eaton's equation can be expressed as follows:

$$\left(\frac{\Delta t_n}{\Delta t}\right)^x = \frac{22.33 - G_p}{(22.33 - 10.5)} \tag{10}$$

$$x = \frac{log\left(\frac{22.33 - G_p}{22.33 - 10.5}\right)}{log\left(\frac{\Delta t_n}{\Delta t_o}\right)} \tag{11}$$

Determining a pressure gradient overlay simplifies the pore pressure determination. It needs to determine Eaton's pore pressure exponent (x). This parameter is determined using a known abnormal pore pressure data from an offset well. The normal sonic transit time (Δt_n) is detected by extrapolating the normal trend line to this abnormal pressure point. Using Equation 11 and a known abnormal pore pressure data from an offset well, Eaton's exponent is determined as 1.46. In order to create the pore pressure overlay, at a given depth (2700 m), the abnormal pore pressure values in 1 kPa/m increments were assumed to be 9, 10, 11, 12, 13, 14, 15, and 16 kPa/m and solved for the observed value of the parameter of interest. Table 1 shows the calculation of these observed transient time values (Δt_o). These observed values associated with the respective increments of pore pressure are detected and trend lines are drawn through them parallel to the normal trend line established. Thus the pore pressure overlay is created and used in pore pressure determination as illustrated in Figure 4. The result of the estimated pore pressure is compared with the average mud pressure data in Figure 8. This figure displays that the predicted pressure values from the model (Weakley's approach) are in good agreement with the average mud pressure data. The difference in correlation with pressure points at some intervals, especially in the range of 3250-3450 m, is probably due to the high permeability at these depths. High permeability can create a hydrodynamic relationship with the adjacent formation pressure. It makes a constant pore pressure gradient in these intervals, which may differ from the estimated pore pressure.

Table 1

Calculation of the observed transient time values in different pore pressure gradients.

Eaton's Equation	Point	G_p (kPa/m)	Δt_o (µs/m)
$\Delta t_o = \dfrac{\Delta t_n}{\left(\dfrac{G_o - G_p}{G_o - G_n}\right)^{\frac{1}{x}}}$	A	9	209
	B	10	221
	C	11	234
	D	12	249
$\Delta t_o = \dfrac{227}{\left(\dfrac{22.33 - G_p}{22.33 - 10.5}\right)^{\frac{1}{1.46}}}$	E	13	267
	F	14	289
	G	15	315
	H	16	348

The calculation of pore pressure from other methods like Eaton's or Bowers's is possible with some assumptions, but it needs some geological study before applying. It should be noted that each of these methods relies on a consideration that the overpressure is resulting from a specific mechanism as the main factor of overpressure and it provides an empirical formula for the estimation of pore pressure. Therefore, choosing each method is reasonable based on geological studies, which lead to understanding the overpressure generation mechanism and choosing the appropriate pore pressure prediction method. For this purpose, porosity related well-log data, including sonic and density are used to determine the overpressure generation mechanism and the appropriate pore pressure prediction method.

Density logs represent the bulk properties of the rock and sonic logs represent the transport properties of the rock. Katsube et al. (1992) considered the porosity of the rock as a combination of connected pores and storage pores. The effectiveness of the bulk properties in response to the neutron porosity and density logs is the same, but the effectiveness of the transport properties of the rock in response to sonic and resistivity logs is higher for connected pores. Bowers and Katsube (2002) used the

difference in bulk and transport properties as a detection factor for overpressure generation mechanism. Bowers used the velocity-density cross plot to identify the overpressure resulted from compaction disequilibrium and unloading mechanism.

Compaction disequilibrium mechanism has the same effect on both storage and connected pores. Hence bulk and transport properties should be equally responsive to overpressure caused by compaction disequilibrium and the sonic and density logs will show similar changes in trends. When pore pressure increases due to fluid expansion, the unloading response is essentially elastic and results in only a very small increase in porosity. This increase in porosity is predominantly due to the opening of flat connecting pores, or microcracks, because they are more compliant than the storage pores. As the density log measures the bulk porosity, it is barely affected by this effect. However, the sonic and resistivity log responses are sensitive to the opening of connecting pores due to an increase in conductivity. Hence the sonic and density logs will show mismatches.

Therefore, the compaction disequilibrium can slow down or arrest the velocity-density cross plot, but the unloading mechanism creates a return trend below the graph. The velocity-density cross plot (with depth classified based on color) of a well located in the studied area is shown in Figure 5. It shows that an increase in velocity-density cross plot is arrested at overpressure depths (3200-3600 m) and no return trend can be seen below the graph. Moreover, the velocity-density cross plot is in good agreement with the normal compaction trends from Gardner (based on shale) and Anselmetti (based on carbonate) relationships. The observed evidence shows that the overpressure is higher due to compaction disequilibrium.

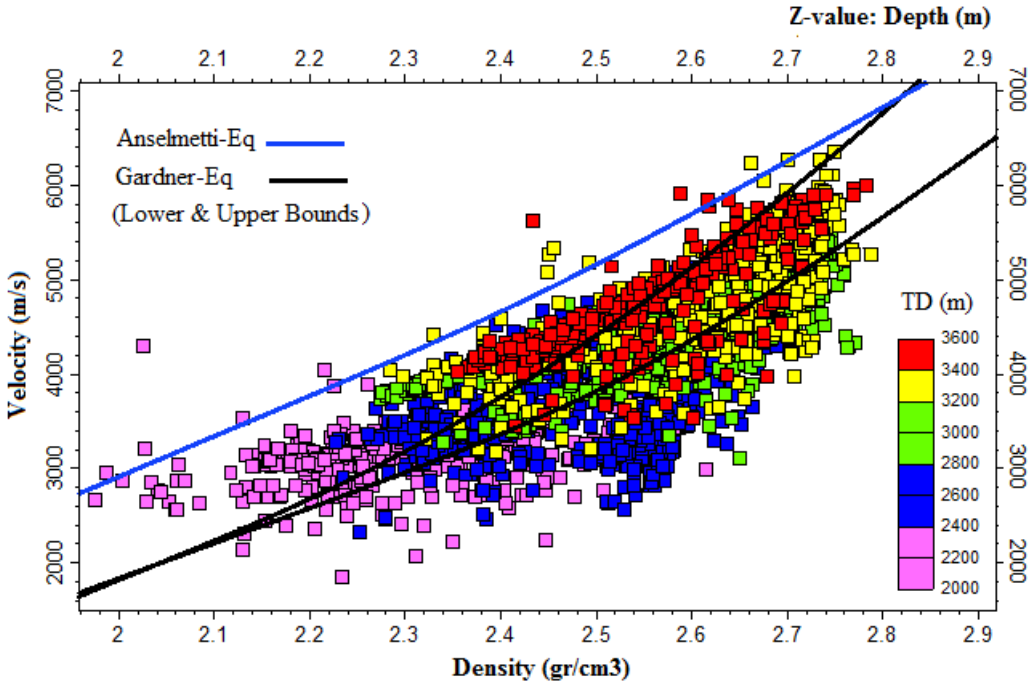

Figure 5
Velocity versus density; normal compaction trends from Gardner and Anselmetti relationships for velocity-density cross plot in shales (Gardner) and carbonate (Aselmetti) are also shown.

Eaton's method and the simple form of Bowers's method, which consider the compaction disequilibrium as the main mechanism of abnormal pressure, can be used in pore pressure determination. In Eaton's method, the first step is to detect the normal compaction trend line based on

shale points in the normally compacted section of the well log data (less than 3100 m), as shown in Figure 6. The normal compaction trend (NCT) of the transit time is proposed by:

$$\Delta t_n(\mu s/m) = 660 \times e^{-0.00039 \times z} \tag{12}$$

where, z is the depth in meters. Substituting Equation 12 into Equation 2 and using the pervious overburden and hydrostatic pressure gradient, the Eaton's sonic equation can be expressed by:

$$G_p = 22.33 - (22.33 - 10.5)\left(\frac{660 \times e^{-0.00039 \times z}}{\Delta t_o}\right)^x \tag{13}$$

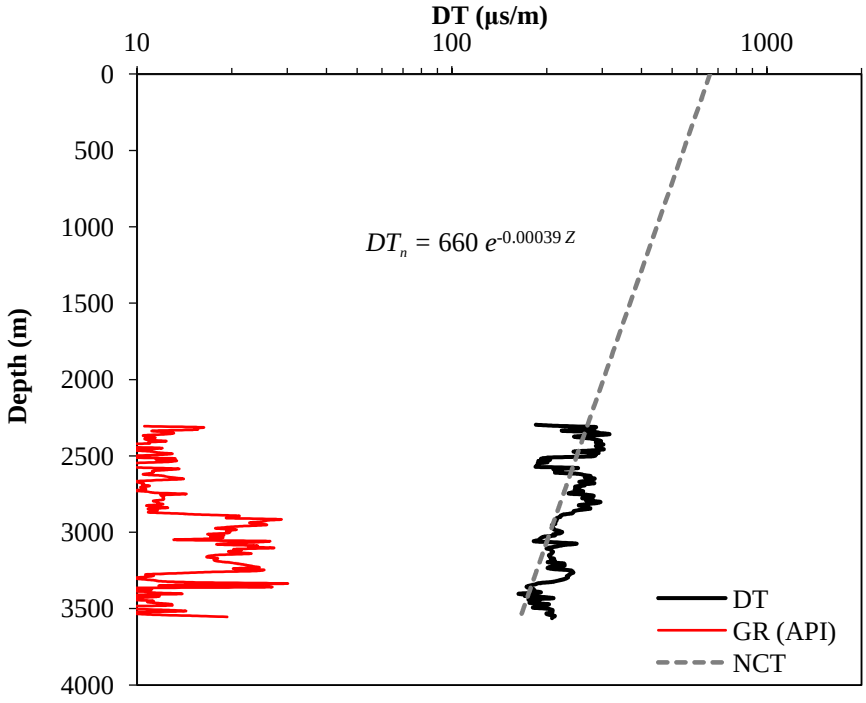

Figure 6
Normal compaction trend line (NCT) corresponding to shale points in normal pressure intervals and DT_0=660 µs/m.

Using Eaton's exponent x=0.8, pore pressure is calculated as depicted in Figure 8.

In Bowers's method, sonic velocity should be related to effective stress based on well data in normally pressured intervals. In this way, the effective stress was calculated using Terzaghi's equation and overburden and hydrostatic pressure gradients were then computed. Next, a graph of velocity versus effective stress for an offset well was built from data points in normal pressure intervals as shown in Figure 7. The best-fit function was calculated based on Equation 3 as reads:

$$V - 1500 = 24.046\,\sigma^{1.3066} \tag{14}$$

Using the above equation and Terzaghi's relationship, the pore pressure is calculated as shown in Figure 8.

The results obtained from this study are summarized in Figure 8. As shown in Figure 8, the estimated

pore pressure from Eaton's method at depths of 3300-3600 m is lower in comparison with Bowers's and Weakley's outcomes. Bowers's method shows better agreement with the average mud weight pressure data. Eaton's and Bowers's methods underestimate the pore pressure at depths of 2500-2600 m, whereas there is no evidence of change in mud weight pressure. Better fit in some intervals of Weakley's outcome can be due to trend lines recalibration, which leads to compensating the low prediction in this interval. However, a restriction of Weakley's method is that the formation section detection and normal compaction trend need to be interpreted from well-logging data. Therefore, the results obtained from this method are further influenced by the skill and judgment of the interpreter in comparison with the common Eaton's or Bowers's method.

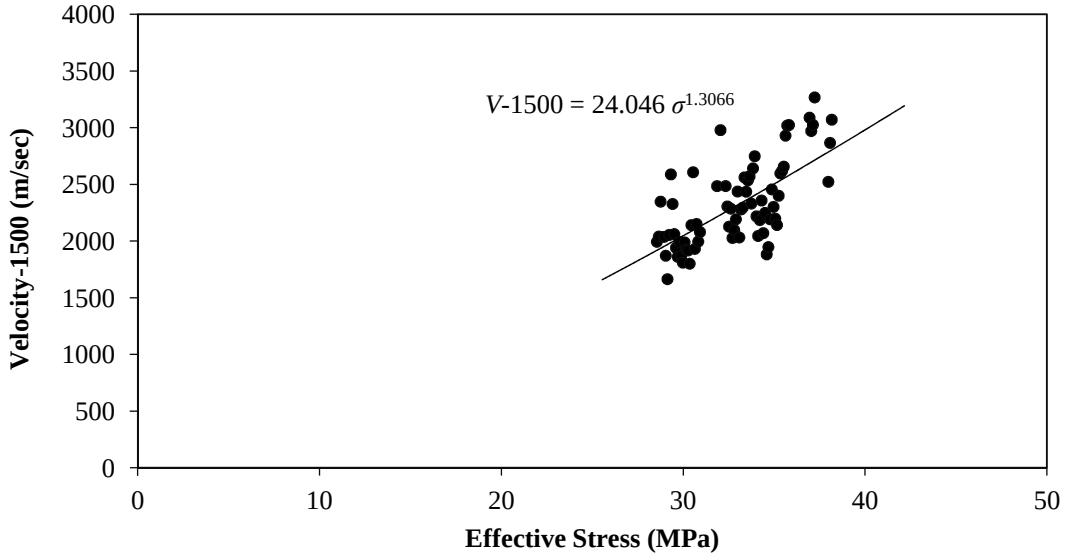

Figure 7
The cross plot of the effective stress versus the V-V_0, where V_0 is the velocity at zero effective stress and is equal to 1500 m/sec.

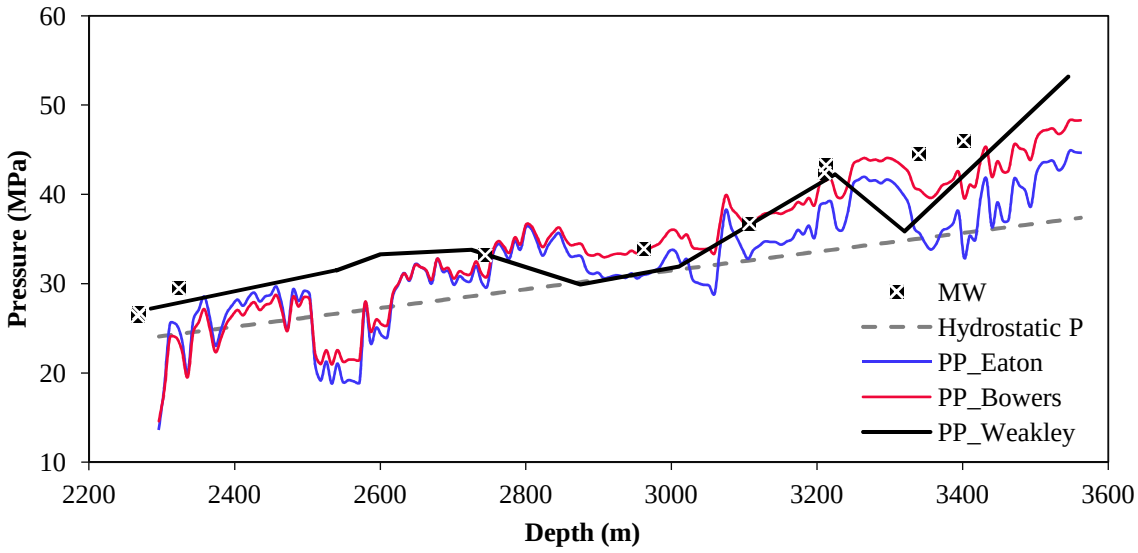

Figure 8
Estimated pore pressure from Weakley's approach and Eaton's and Bowers's methods in comparison with the mud weight pressure.

5. Conclusions

In order to determine formation pore pressure, common well log data are used. According to the results of this study, the following conclusions can be drawn:

1. Pore pressure prediction and modeling based on sonic well-log provide acceptable results in the studied carbonate formation;
2. Analyzing the results of Weakley's approach in the estimation of pore pressure indicates that this method can provide better correlations in comparison with Eaton's method in the studied oil field, but the best agreement with the average mud weight pressure data is provided by Bowers's method;
3. Eaton's equation with an exponent coefficient of 1.46, in Weakley's approach, and 0.8, in the main Eaton's method, gives the best correlation with mud weight pressure values;
4. Weakley's approach is more influenced by the skill and judgment of the interpreter in comparison with the usual method of Eaton.

Nomenclatures

A, B	: Bowers's constant parameters
C_b	: Bulk compressibility (psi^{-1})
C_p	: Pore compressibility (psi^{-1})
G_n	: Normal pressure gradient (MPa/km)
G_o	: Overburden pressure gradient (MPa/km)
G_p	: Pore pressure gradient (MPa/km)
P	: Pore pressure (MPa)
S	: Overburden pressure (MPa)
U	: Unloading parameter
V	: Velocity (m/s)
V_0	: Velocity at the surface (m/s)
V_{max}	: Maximum velocity (m/s)
x	: Eaton's exponent
z	: Depth (m)
β	: Compaction strain-hardening coefficient
ΔT_n	: Normal sonic transit time (μs/m)
ΔT_o	: Measured sonic transit time (μs/m)
$\emptyset$	: Porosity (fraction)
σ	: Vertical effective stress (MPa)
σ_{max}	: Maximum vertical effective stress (MPa)
χ	: Compressibility method exponent

References

Anselmetti, Flavio, S., and Gregor, P. Eberli, Controls on Sonic Velocity in Carbonates, Pure and Applied Geophysics, Vol. 141, No. 2-4, p. 287-323, 1993.

Atashbari, V. and Tingay, M., Pore Pressure Prediction in Carbonate Reservoirs, in SPE Latin America and Caribbean Petroleum Engineering Conference, 2012.

Azadpour, M., Shad Manaman, N., Kadkhodaie-Ilkhchi, A., and Sedghipour, M.R., Pore Pressure Prediction and Modeling using Well-logging Data in One of the Gas Fields in South of Iran, Journal of Petroleum Science and Engineering, Vol. 128, p. 15-23, 2015.

Bowers, G., Pore Pressure Estimation from Velocity Data: Accounting for Overpressure Mechanisms Besides Undercompaction, SPE Drilling & Completion, Vol. 10, No. 2, p.89-95, 1995.

Bowers, G. and Katsube, T. J., The Role of Shale Pore Structure on the Sensitivity of Wire-line Logs to Overpressure, AAPG Memoir, Vol. 76, p. 43-60, 2002.

Contreras, OM, Tutuncu, AN., Aguilera, RM., and Hareland, GM., a Case Study for Pore Pressure Prediction in an Abnormally Sub-pressured Western Canada Sedimentary Basin, in 45th US Rock Mechanics/Geomechanics Symposium, 2011.

Eaton, B., the Equation for Geopressure Prediction from Well Logs, in Fall Meeting of the Society of Petroleum Engineers of AIME, 1975.

Holbrook, P., A Simple Closed Form Force Balanced Solution for Pore Pressure, Overburden and the Principle Stresses, Earth Marine and Petroleum Geology, Vol. 16, p.303-319, 1999.

Hottmann, CE. and Johnson, RK., Estimation of Formation Pressures from Log-derived Shale Properties, Journal of Petroleum Technology, Vol. 17, No. 06, p.717-722, 1965.

Katsube, T., Williamson, M., and Best M., Shale Pore Structure Evolution and its Effect on Permeability, 33th Annual Symposium of the Society of Professional Well Log Analysts (SPWLA), Symposium, p. 1-22, 1992.

Swarbrick, B. E. and Osborne, M. J., Mechanisms that Generate Abnormal Pressures, an Overview, Memoirs-American Association of Petroleum Geologists, p. 13-34, 1998.

Terzaghi, K., Theoretical Soil Mechanics, 1943.

Weakley, R. R., Determination of Formation Pore Pressures in Carbonate Environments from Sonic Logs, in Annual Technical Meeting, Petroleum Society of Canada, 1990.

Zhang, J., Pore Pressure Prediction from Well Logs, Methods, Modifications, and New Approaches, Earth-science Reviews, Vol. 108, No. 1, p. 50-63, 2011.